

AN IMPROVED [O III] LINE WIDTH TO STELLAR VELOCITY DISPERSION CALIBRATION: CURVATURE, SCATTER, AND LACK OF EVOLUTION IN THE BLACK-HOLE MASS VERSUS STELLAR VELOCITY DISPERSION RELATIONSHIP

C. MARTIN GASKELL

Department of Astronomy, University of Texas, Austin, TX 78712-0259.

Submitted to ApJ

ABSTRACT

An improved transformation of the full width at half maxima (FWHM) of the [O III] $\lambda 5007$ line in AGNs to the stellar velocity dispersion, σ_* , of the host galaxy is given. This significantly reduces the systematic errors in using $\text{FWHM}([\text{O III}])$ as a proxy for σ_* . AGN black hole masses, M_\bullet , estimated using the Dibai single epoch spectrum method, are combined with the new estimates of σ_* to give a revised AGN $M_\bullet - \sigma_*$ relationship extending up to high masses. This shows that for the most massive black holes, M_\bullet is systematically higher than predicted by extrapolation of $M_\bullet \propto \sigma_*^4$ to high masses. This supports recent suggestions that stellar dynamical masses of the most massive black holes have been systematically underestimated. The steepening of the $M_\bullet - \sigma_*$ relationship is consistent with the absence of very high σ_* galaxies in the local universe and with the curvature of the Faber-Jackson relationship. There appears to be significantly less intrinsic scatter in the $M_\bullet - \sigma_*$ relationship for galaxies with $M_\bullet > 10^9 M_\odot$. It is speculated that this is connected with the core elliptical versus extra-light elliptical dichotomy. The low scatter in the high end of the $M_\bullet - \sigma_*$ relationship implies that the transformation proposed here and the Dibai method are good indicators of σ_* and M_\bullet , respectively. There is no evidence for evolution of the $M_\bullet - \sigma_*$ relationship over time.

Subject headings: galaxies:active — galaxies:bulges — galaxies: evolution — galaxies: fundamental parameters — galaxies: nuclei — quasars:emission lines

1. INTRODUCTION

There is considerable interest in the correlation of the masses, M_\bullet , of supermassive black holes (SMBHs) with the stellar velocity dispersion, σ_* , of the bulge of the host galaxy (Gebhardt et al. 2000; Ferrarese & Merritt 2000; Kormendy & Gebhardt 2001) because of its important implications for the formation and evolution of galaxies and their SMBHs. It is widely recognized that for understanding the origin of the $M_\bullet - \sigma_*$ relationship it is particularly important to know the masses of black holes in the most massive and least massive galaxies, and to study the evolution of the $M_\bullet - \sigma_*$ relationship over cosmic time. Having the correct form of the relationship is also important for constructing the black hole mass function in the local universe and reconciling this with the luminosity function of AGNs, energy-generation efficiencies, relative accretion rates (Eddington ratios), AGN duty cycles, and the evolution of all these quantities over the history of the universe. The predictions from the bulge luminosity, L_{bulge} , and from the $M_\bullet - \sigma_*$ relationship conflict for the highest-luminosity galaxies because the $M_\bullet - L_{\text{bulge}}$ relationship predicts that the brightest galaxies have $M_\bullet \sim 10^{10} M_\odot$, while the $M_\bullet - \sigma_*$ relationship predicts $M_\bullet < 3 \times 10^9 M_\odot$ at all times (Bernardi et al. 2007b; Lauer et al. 2007). The number of high-mass SMBHs predicted by the $M_\bullet - \sigma_*$ relationship is also in conflict with the number of relic high-mass SMBHs predicted by the volume density of the most luminous AGNs (Lauer et al. 2007).

By far the easiest way to estimate black hole masses is to use type-1 (near face-on) AGNs. To do this one needs the velocity dispersion of the broad-line

region (BLR) gas, which can be readily obtained from the $\text{H}\beta$ line width, and an effective radius. It is also important to establish that the motions of the gas being used are dominated by gravity. The most direct way of determining an effective radius is via “reverberation mapping” using light echoes following AGN variability (Lyutyi & Cherepashchuk 1972; Cherepashchuk & Lyutyi 1973). This is most readily accomplished by cross correlating line and continuum variability (Gaskell & Sparke 1986). Velocity-resolved light echoes have shown that BLR gas motions are gravitationally dominated (Gaskell 1988; Koratkar & Gaskell 1989; see Gaskell & Goosmann 2008 and Gaskell 2009 for reviews of the evidence for this) and thus permit estimation of M_\bullet from the BLR. Since then, M_\bullet has been estimated from reverberation mapping for several dozen AGNs (see Vestergaard & Peterson 2006 for a recent compilation). An external check on the accuracy of reverberation mapping masses is provided by the tightness of the correlations of the M_\bullet estimates with σ_* and L_{bulge} . The bulge luminosities obtained by Bentz et al. (2009a) imply that the error in $\log M_\bullet$ determined by reverberation mapping is less than ± 0.33 dex.

Reverberation mapping is unfortunately very labor intensive, but Dibai (1977) argued that BLR radii, and hence masses, could be inferred indirectly from photoionization considerations from single-epoch spectra. Mass estimates from a large number of spectra of NGC 5548 in high and low states (Denney et al. 2009) show that random and systematic measuring errors in $\log M_\bullet$ determined by the Dibai method are small (≈ 0.11 dex). Bochkarev & Gaskell (2009) have shown that Dibai’s original mass estimates (Dibai 1977, 1980, 1984) are in good agreement with reverberation-

mapping mass estimates. The same is true for more recent mass determinations by the Dibai method (Vestergaard & Peterson 2006). As with reverberation-mapping-determined masses, an independent external check is provided by correlations with the properties of the host-galaxy bulges. Gaskell & Kormendy (2009) find a scatter of ± 0.23 in $\log M_\bullet$. These studies suggest that, with care, the Dibai method, which is about two orders of magnitude less labor intensive than reverberation mapping, gives M_\bullet accurate to $\lesssim \pm 0.25$ dex.

A problem in investigating the $M_\bullet - \sigma_*$ relationship for AGNs is that strong optical continuum emission from the AGN accretion disk can make measuring σ_* difficult. This is exacerbated as one goes to higher redshifts as the most readily observable stellar absorption lines move into the IR. Nelson (2000) proposed using $\text{FWHM}_{[\text{O III}]} / 2.35$ as a proxy for σ_* because the $[\text{O III}]$ lines are strong and readily observable. For a Gaussian velocity dispersion, $\sigma = \text{FWHM} / 2.35$. By using $\text{FWHM}_{[\text{O III}]} / 2.35$ Nelson showed that active galaxies also obey the $M_\bullet - \sigma_*$ relationship. The use of $\text{FWHM}_{[\text{O III}]}$ as a proxy for σ_* has subsequently been widely adopted because the $[\text{O III}]$ lines are readily observable and they allow studies of the $M_\bullet - \sigma_*$ relationship to be extended to higher redshifts and higher luminosities (Shields et al. 2003).

An obvious concern with using $\text{FWHM}_{[\text{O III}]}$ as a proxy for σ_* is that gas, unlike stars, is highly susceptible to non-gravitational forces and dissipation, and it has long been known that the motions of the gas in galaxies are complicated. In this paper I show that using $\text{FWHM}_{[\text{O III}]}$ as a proxy for σ_* *underestimates* σ_* for narrow $[\text{O III}]$ lines and *overestimates* it for broad $[\text{O III}]$ lines. I give a simple prescription for removing this bias, and discuss the implications for the $M_\bullet - \sigma_*$ relationship.

2. USING THE FWHM OF $[\text{O III}]$ AS A PROXY FOR STELLAR VELOCITY DISPERSION

The justification of Nelson (2000) in using $\text{FWHM}_{[\text{O III}]} / 2.35$ as a proxy for σ_* was that in the compilation of Nelson & Whittle (1995) and Nelson & Whittle (1996), the *average* $\text{FWHM}_{[\text{O III}]} / 2.35$ was in good agreement with their average directly measured σ_* . A number of other studies (e.g., Boroson 2003; Onken et al. 2004; Greene & Ho 2005; Bonning et al. 2005) have supported the use of $\text{FWHM}_{[\text{O III}]} / 2.35$ as a proxy for σ_* , although one with significant scatter. This scatter is not surprising as it has long been known (Burbidge, Burbidge, & Prendergast 1959) that the narrow emission lines are blueshifted and this has been shown in a number of cases to be the result of outflow. The widths of the narrow-line region (NLR) lines also depend on the ionization potential and critical densities of the lines (de Robertis & Osterbrock 1986), so different lines will give systematically different FWHMs. With these complications we therefore expect a merely empirical correlation between $\text{FWHM}_{[\text{O III}]} / 2.35$ and σ_* at best.

Fig. 1 shows $\text{FWHM}_{[\text{O III}]} / 2.35$ and measured σ_* values from Nelson & Whittle (1995) and Nelson & Whittle (1996). Additional or updated σ_* measurements were taken from Nelson (2000) (Mrk 79, Mrk 110, Mrk 279), Nelson et al. (2004) (NGC 4151 and NGC 5548), and Onken et al. (2004) (NGC 7469, Mrk 817, Ark 120).

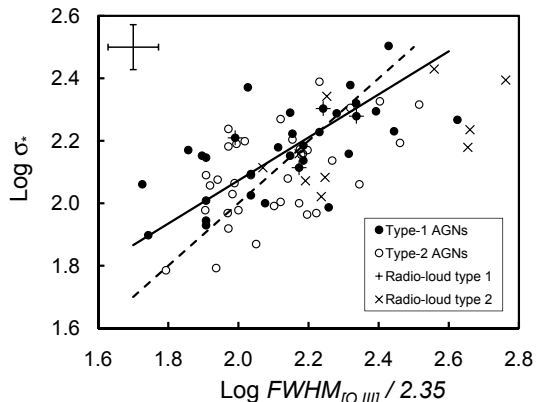


FIG. 1.— Measured stellar velocity dispersion, σ_* , as a function of $\text{FWHM}_{[\text{O III}]} / 2.35$ for AGNs. The dotted line is the equation $\sigma_* = \text{FWHM}_{[\text{O III}]} / 2.35$ and the solid line is an OLS-bisector fit (Isobe et al. 1990) for the type-1 AGNs only.

Updated $\text{FWHM}_{[\text{O III}]}$ measurements were taken from Nelson (2000) for NGC 7469, Mrk 79, Mrk 110, Mrk 279, Mrk 817, and Ark 120. Strong radio sources (objects in Table 7 of Nelson & Whittle 1995) are indicated by the addition of a “+” to type-1 objects and a “x” to type-2 objects.

It can be seen from Fig. 1 that while $\text{FWHM}_{[\text{O III}]} / 2.35$ for all AGNs agrees on average with σ_* for the sample as a whole, there is substantial scatter. Nelson & Whittle (1996) find an rms scatter of ± 0.20 dex (see their Fig. 7a). The rms scatters for both the type-1 and type-2 AGNs in Fig. 1 are similar (± 0.20 dex ± 0.19 dex respectively). The rms of the quoted measuring errors of σ_* is ± 0.07 dex. Comparison of FWHMs of $[\text{O III}]$ with the FWHMs of similar ionization $[\text{S III}]$ lines (Table 3 of Nelson & Whittle 1995) suggests that the rms error in the measurement of each line is ± 0.06 dex. The expected scatter in Fig. 1 from measuring errors alone is thus expected to be $\approx \pm 0.10$ dex.

In addition to the large scatter in Fig. 1, it can be seen that there is a *systematic* deviation from $\sigma_* = \text{FWHM}_{[\text{O III}]} / 2.35$ for wide $[\text{O III}]$ lines as has already been noted by Nelson & Whittle (1996). It is, of course, important for studying the $M_\bullet - \sigma_*$ relationship for AGNs that there be no systematic errors in estimating σ_* . Nelson & Whittle (1996) have already pointed out that the systematic deviation is strongest for radio-loud AGNs. Fig. 1 shows that it is actually the *type-2* radio-loud AGNs which show the largest systematic effect. This argues that the NLR outflows are preferentially near the equatorial plane. Type-1 AGNs show a similar systematic bias when $[\text{O III}]$ is used as a proxy for σ_* . This is shown by the OLS-bisector fit (Isobe et al. 1990) to the type-1 AGNs alone in Fig. 1. The effect is quite substantial. For type-1 AGNs with $\text{FWHM}_{[\text{O III}]} / 2.35 < 100 \text{ km s}^{-1}$ the median under prediction of σ_* is 0.22 dex. Since $M_\bullet \propto \sigma_*^4$, this translates into a 0.9 dex systematic error $\log M_\bullet$.

The NLR line widths are consistent with other observations showing that emission-line gas velocities in bulges tend to be sub-virial. For example, in a large study of elliptical galaxies by Phillips et al. (1986) the mean $\text{FWHM} / 2.35 / \sigma_*$ from their $[\text{N II}]$ FWHMs is 0.73 ± 0.03 . Spatially resolved *Hubble Space Telescope* spectroscopy of

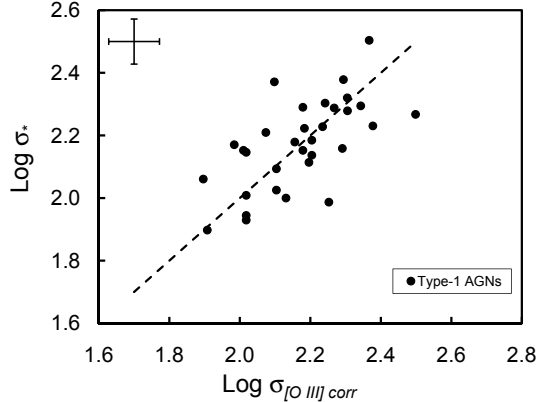


FIG. 2.— Measured stellar velocity dispersion, σ_* , as a function of the corrected [O III] line velocity dispersion, $\sigma_{[\text{O III}] \text{corr}}$, from Eq. 1. The diagonal line is the equation $\sigma_* = \sigma_{[\text{O III}] \text{corr}}$.

NLRs shows that the innermost gas is commonly moving more slowly than gas further out (Rice et al. 2006).

Sub-virial NLR motion is obviously being seen because gas is settling into a flattened distribution. Since type-1 AGNs are viewed close to face-on, this will reduce the observed FWHM for gas in a flattened distribution. The smaller systematic offset for type-2 AGNs would be because they are viewed more obliquely. It can be seen in Fig. 1 that both the overestimation of σ_* and the difference between type-1 and type-2 AGNs decreases as the FWHM gets wider. The reason for the decreasing difference between type-1 and type-2 AGNs with increasing FWHM could be that for type-1 AGNs with the largest FWHMs the torus opening angle is larger than average, and so they can be seen at higher inclinations. The extra width of [O III] could also be associated with an outflow. This must certainly be going on for the AGNs with the highest [O III] FWHMs.

3. AN IMPROVED RELATIONSHIP BETWEEN [O III] FWHM AND σ_*

Whatever the cause of the systematic deviations in Fig. 1, it is possible to remove the systematic effect empirically by using a non-linear transformation from $\sigma_{[\text{O III}] \text{corr}}$ to σ_* . For type-1 AGNs a corrected estimate of the velocity dispersion can be defined by the equation:

$$\log \sigma_{[\text{O III}] \text{corr}} = (0.67 \pm 0.09) \log[\text{FWHM}_{[\text{O III}]} / 2.35] + (0.74 \pm 0.02) \quad (1)$$

where the coefficients have been chosen so that an OLS-bisector fit to σ_* and $\sigma_{[\text{O III}] \text{corr}}$ gives the equation $\sigma_* = \sigma_{[\text{O III}] \text{corr}}$. The comparison between the measured σ_* values and the estimates using Eq. 1 are shown in Fig. 2. The scatter for the type-1 AGNs has been reduced to ± 0.12 dex. Type-2 AGNs cannot be used to get M_\bullet via the Dibai method and hence will not be considered further, but the corresponding transformation for type-2 AGNs has a slope of 0.82 ± 0.11 . This is consistent with the slope of Eq. 1, but there is an offset of 0.06 dex in the sense that Eq. 1 would slightly over predict σ_* for type-2 AGNs. For radio-quiet type-2 AGNs the scatter is reduced to ± 0.12 dex, and even for radio-loud AGNs it is reduced to ± 0.14 dex.

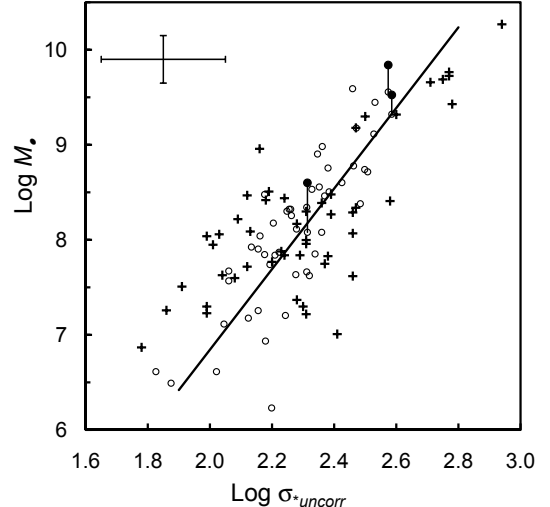


FIG. 3.— The $M_\bullet - \sigma_*$ relationship for the radio-quiet AGNs of Shields et al. (2003) (shown as crosses) and for the non-BLR mass estimates compiled by Gültekin et al. (2009) (shown as open circles). For the Shields et al. (2003) AGNs σ_* has been taken simply to be $\text{FWHM}_{[\text{O III}]} / 2.35$ with no correction. The solid circles joined with short vertical lines to the open circles below them represent the M_\bullet revisions of Humphrey et al. (2008), Gebhardt & Thomas (2009), and van den Bosch (2008). A typical error bar for the AGNs is shown at the upper left. The error in $\sigma_{* \text{uncorr}}$ is the scatter found by Nelson & Whittle (1995), and the error in M_\bullet has been taken to be ± 0.25 following Bochkarev & Gaskell (2009). The diagonal line is the Gültekin et al. (2009) fit.

4. THE $M_\bullet - \sigma_*$ RELATIONSHIP FOR AGNS

Shields et al. (2003) made estimates of M_\bullet and σ_* for a large sample of AGNs with observations by Brotherton (1996a,b), Grupe et al. (1999), McIntosh et al. (1999), Dietrich et al. (2002), and themselves. This sample has an advantage over the nearby AGN sample of Greene & Ho (2006) in having AGNs covering the upper end of the relationship defined by normal galaxies (see Gültekin et al. 2009). Shields et al. (2003) calculated black hole masses from FWHMs of $\text{H}\beta$ by the Dibai method, and σ_* was just taken to be $\text{FWHM}_{[\text{O III}]} / 2.35$. Details of the treatment of the data can be found in Shields et al. (2003). Fig. 3 shows the $M_\bullet - \sigma_*$ relationship for these BLR blackhole mass estimates and also for the non-BLR blackhole mass estimates compiled by Gültekin et al. (2009). For three galaxies revised masses are also shown (see discussion below). M_\bullet estimates from BLR kinematics have always been normalized to the stellar-dynamical $M_\bullet - \sigma_*$ relationship. The Shields et al. (2003) masses have been renormalized to the updated Gültekin et al. (2009) relationship. The renormalization has been made over the range $2.0 < \log \sigma_{[\text{O III}] \text{corr}} < 2.4$ where the corrections to the [O III] estimates of σ_* are smallest (see Fig. 1). The Shields et al. (2003) masses need to be decreased by 0.11 dex to minimize their median residual from the Gültekin et al. (2009) line in this range. This small renormalization has a negligible effect on the results.

It can be seen from Fig. 3 that the Shields et al. (2003) objects deviate systematically from the relationship given by the Gültekin et al. (2009) galaxies. For $\log \sigma_{* \text{uncorr}} < 2.2$ the inferred masses of the Shields et al. (2003) galaxies all lie above the Gültekin et al. (2009) fit,

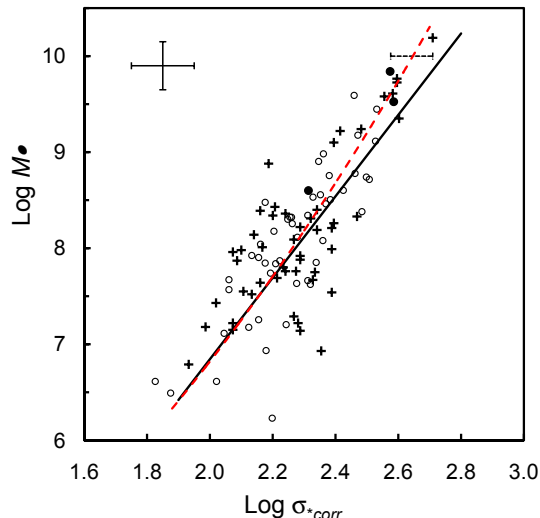


FIG. 4.— The $M_{\bullet}-\sigma_{*}$ relationship for the BLR and non-BLR mass estimate samples as in Fig. 3 but with correction of the stellar velocity dispersion estimates for the AGNs as described in the text. For clarity the three older mass estimates in Fig. 1 that have new values have been omitted. The dashed red curve is Eq. 2. The dashed horizontal error bar in the upper right indicates the effect of the uncertainty in the slope in Eq. 1. All other symbols have the same meaning as in Fig. 3. The error in $\log \sigma_{*corr}$ has been taken to be the scatter in Fig. 2.

and for $\log \sigma_{*uncorr} > 2.7$ they all lie below.

Fig. 4 plots the Shields et al. (2003) galaxies with the corrected estimates of the stellar velocity dispersions given by Eq. 1. It can be seen that the scatter is less and the systematic differences from the Gültekin et al. (2009) points are reduced. The agreement is particularly good at the high-mass end. The typical error bar (upper left corner) is now smaller. The uncertainty in the slope of Eq. 1 introduces an additional uncertainty in σ_{*} for the highest and lowest mass black holes. The amplitude of this uncertainty for a typical high-mass black hole is indicated by the horizontal error bar at the upper right. One of the free parameters in the Dibai method is the slope of the relationship between the effective radius, R , of the BLR and the optical luminosity, L_{AGN} . This introduces an additional uncertainty in the $M_{\bullet}-\sigma_{*}$ relationship for high- and low-mass AGNs. Shields et al. (2003) took $R \propto L^{0.5}$. This is in good agreement with the best current estimate of $R \propto L^{0.52}$ (Bentz et al. 2009b).

5. DISCUSSION

5.1. The masses of the most massive black holes

The revised AGN $M_{\bullet}-\sigma_{*}$ relationship of Fig. 4 supports recent upwards revisions of stellar dynamical M_{\bullet} estimates in massive galaxies. Two effects are responsible for the revisions. The first is that including dark halos in stellar dynamical modelling of the most massive galaxies (see Gebhardt & Thomas 2009) increases the estimated masses of their black holes by about a factor of two. The masses of two of the most massive black holes have been increased already (see Fig. 3), and more masses of the most massive black holes are expected to increase similarly (K. Gebhardt - private communication). The second effect is that triaxial orbit calculations can give a higher M_{\bullet} than axisymmetric models. This has been demonstrated for NGC 3379 by van den Bosch (2008) and van den Bosch et al. (2009). This is likely

to be a general effect and triaxial galaxies are believed to dominate among high-mass galaxies. The two systematic effects are independent and are expected to act together for some high-mass galaxies. Further upward revisions of the masses of the most massive black holes are thus likely. Some support for this already comes from direct measurement of σ_{*} in AGNs with black hole masses determined from reverberation mapping. For some of the AGNs with $\log \sigma_{*} \sim 2.3$ their masses can be up to ~ 0.7 dex above the stellar dynamical $M_{\bullet}-\sigma_{*}$ relationship (Dasyra et al. 2007; Watson et al. 2008; Woo et al. 2008).

5.2. Curvature in the $M_{\bullet}-\sigma_{*}$ relationship

It can be seen from Fig. 4 that for both the Gültekin et al. (2009) galaxies and the Shields et al. (2003) AGNs, the Gültekin et al. fit underpredicts $\log M_{\bullet}$ by about 0.5 dex for galaxies with $\log M_{\bullet} > 9$. Even before the recent upwards revision of mass estimates of the highest mass black holes (see previous section), Wyithe (2006) had argued that a curved log-quadratic relationship was a better fit to the $M_{\bullet}-\sigma_{*}$ relationship than a simple power-law. Hu (2008) also suggests upwards curvature of the relationship at the high-mass end.

It is now recognized that the shape of the $M_{\bullet}-\sigma_{*}$ relationship depends on the type of galaxy being looked at (Graham 2008; Hu 2008). Defining the form of the relationship for a mixed sample of galaxies is particularly problematic at the lower end. It will take further work to establish the true shape of the top of the $M_{\bullet}-\sigma_{*}$ relationship for AGNs, but if we assume that the Gültekin et al. (2009) line is a good representation for $\log \sigma_{*} \lesssim 2.5$, then the median slope of a power law from $\log \sigma_{*} = 2.5$ to the top ten points in Fig. 4 is 5.5. For computational convenience in interpreting observations, these two lines can be approximated by the log-quadratic:

$$\log M_{\bullet} = 1.1(\log \sigma_{*})^2 - 0.2 \log \sigma_{*} + 2.82 \quad (2)$$

It should be noted that, for the points in Fig. 4, the reduction in χ^2 per degree of freedom in going from a power-law to a log-quadratic relationship is not significant. Gültekin et al. (2009) get a similar result for their galaxies alone. This is because of the scatter in the lower half of the relationship. Whether or not a log-quadratic curve is formally needed depends on the choice of low σ_{*} galaxies included. The significant thing about Fig. 4, however, is that the slope of the $M_{\bullet}-\sigma_{*}$ relationship at the high-mass end is steeper than in the Gültekin et al. (2009) fit and similar previous fits (e.g., Tremaine et al. 2002).

Since the determination of the slope of the upper part of the $M_{\bullet}-\sigma_{*}$ relationship (see above) depends in part on stellar dynamical mass estimates, some of which are expected to increase (see section 5.2), the slope of the top of the relationship could well increase further. Even though curvature in the $M_{\bullet}-\sigma_{*}$ relationship is currently only marginally statistically significant (see discussion in Gültekin et al. 2009), there are good reasons to believe that the relationship *must* curve upwards strongly. This is because it has long been known (Oegerle & Hoessel 1991) that the relationship between galaxy luminosity and σ_{*} (Faber & Jackson 1976) curves strongly at the high-luminosity end and σ_{*}

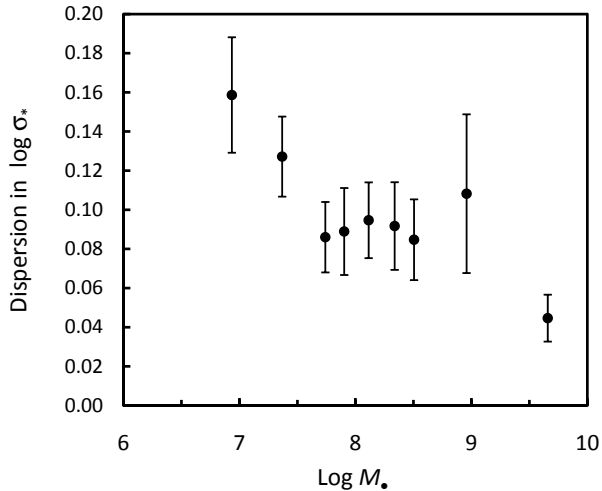


FIG. 5.— The dispersion $\log \sigma_*$ (in standard deviations) as a function of $\log M_{\bullet}$. The bins have been chosen to have equal numbers of objects.

saturates. The highest velocity dispersion galaxies found by (Oegerle & Hoessel 1991) have $\log \sigma_* \sim 2.6$, and further searches have failed to turn up any galaxies with $\log \sigma_* > 2.65$ (Salviander et al. 2008). The velocity dispersions for the most massive black holes in Fig. 4 are consistent with this limit. The steepening in Fig. 4 removes the discrepancy between the $M_{\bullet}-\sigma_*$ and $M_{\bullet}-L_{bulge}$ relationships (Bernardi et al. 2007b; Lauer et al. 2007), and as Wyithe (2006) points out, the steepening increases the local density of the highest mass black holes.

5.3. Dispersion in the $M_{\bullet}-\sigma_*$ relationship as a function of M_{\bullet}

Another interesting thing in Fig. 4 is the tightness of the $M_{\bullet}-\sigma_*$ relationship at the high-mass end. This impression is confirmed in Fig. 5 which shows the dispersion in $\log \sigma_*$ for the combined samples in Fig. 4 as a function of $\log M_{\bullet}$. It can be seen that the dispersion for the highest-mass objects is significantly lower than for the remaining objects. An F-test gives a probability, $p = 0.01$ that the dispersions of objects with $M_{\bullet} > 10^9$ and $10^{7.5} < M_{\bullet} < 10^9 M_{\odot}$ are drawn from the same parent population. The decrease in dispersion at high masses is seen for the BLR estimates and the Gültekin et al. 2009 estimates separately, but at lower significance.

The scatter at the lower end of the $M_{\bullet}-\sigma_*$ relationship is similar to that found by Greene & Ho (2006) from direct measurements of the stellar velocity dispersion by for AGNs with BLR masses determined by the Dibai method. It is also similar to that found by Onken et al. (2004) for reverberation-mapped AGNs with a mixture of direct measurements of stellar velocity dispersions and estimates from $\text{FWHM}_{[OIII]}/2.35$. In Fig. 1 of Greene & Ho (2006) the increase in scatter going from the high-mass galaxies with stellar dynamical determinations to the lower-mass AGNs is particularly striking. The results presented here argue that this effect is real and not a consequence of larger measuring errors for the AGNs.

The increase in scatter in the $M_{\bullet}-\sigma_*$ relationship as one goes to lower black hole and galaxy masses probably tells us something about blackhole growth associated with the different processes that dominate the evolution of galaxies of different masses. Elliptical galaxies and classical bulges in spirals are the result of violent mergers. For lower mass galaxies, secular evolution dominates instead. Secular evolution can be recognized by the presence of bars, pseudobulges, and other features (see Kormendy & Kennicutt 2004). It is now known that galaxies with bars and pseudo-bulges have systematically lower blackhole masses than predicted by the $M_{\bullet}-\sigma_*$ relationship for ellipticals and classical bulges (Hu 2008; Graham 2008). Secular evolution must therefore be a cause of some of the increase in scatter in Fig. 5. One test of whether it is the *only* cause of the trend is to look at the dispersion in $\log \sigma_*$ for the pure ellipticals. Inspection of the ellipticals in the Gültekin et al. sample shows that the dispersion rises from ≈ 0.05 dex at $\log M_{\bullet} \approx 9.5$ to ≈ 0.11 at $\log M_{\bullet} \approx 7.5$. Unfortunately, the significance of this trend is low ($p = 0.25$) because of the small sample size. If the dispersion does indeed rise for the lowest mass ellipticals, this would suggest that secular evolution at low masses is *not* the only cause of the dependence of dispersion on black hole mass.

For the highest mass galaxies the low dispersion in $M_{\bullet}-\sigma_*$ is probably associated with the dichotomy between ellipticals with “cores” and those with central “extra light” (Kormendy et al. 2009). “Core” ellipticals have had their cores scoured out by supermassive black hole binaries (Ebisuzaki et al. 1991) after “dry” dissipationless mergers. “Extra-light” ellipticals have had major star formation in their centers following “wet” starburst mergers. Ellipticals with $M_{\bullet} > 10^9$ are core ellipticals. Bernardi et al. (2007a) have shown that the brightest ellipticals have a very low scatter in the fundamental plane, and Kormendy & Bender (2009) have shown that core ellipticals have a tight correlation between σ_* and the stellar light deficit. All these things and the lower dispersion in the $M_{\bullet}-\sigma_*$ relationship point to core ellipticals having very uniform properties.

5.4. Evolution of the $M_{\bullet}-\sigma_*$ relationship

The radio-quiet AGNs in the Shields et al. (2003) sample go up to a redshift of 3.286. Shields et al. (2003) claimed that deviations from the $M_{\bullet}-\sigma_*$ relationship as a function of redshift showed that the relationship was unchanged out to $z \approx 3$ and hence consistent with the growth of massive bulges and black holes occurring simultaneously. The results presented here support this conclusion even though the analyzes are different. Shields et al. (2003) used uncorrected estimates of σ_* (see Fig. 3) which, as discussed above, are systematically too high for the most massive AGNs. To look for evolutionary effects Shields et al. (2003) looked for a redshift dependence in residuals from the Tremaine et al. (2002) $M_{\bullet}-\sigma_*$ relationship. The slope of this relationship is somewhat flatter than the Gültekin et al. (2009) slope (4.02 versus 4.24) and significantly flatter than the slope of 5.5 for the upper end of the relationship in Fig. 4. The flatter slope Shields et al. (2003) adopted for the $M_{\bullet}-\sigma_*$ relationship compensated for the larger estimates of σ_* at high masses.

Although the overall $M_{\bullet}-\sigma_*$ relationship seems sim-

ilar at low and high redshifts much work needs to be done. The relationship really needs to be compared, not for heterogeneous collections of galaxies, but for different evolutionary stages of galaxies that will end up similar. Although there does not seem to be strong evolution of the very highest mass galaxies and their black holes, strong evolution of lower mass galaxies and black holes is quite possible (Woo et al. 2008), since there is more scatter in the $M_{\bullet}-\sigma_{*}$ relationship. In studying evolution, however, care needs to be taken to allow for selection biases (see for example Salviander et al. 2007).

6. CONCLUSIONS

An improved transformation of $\text{FWHM}_{[O III]}$ to σ_{*} has been proposed. This makes the velocity dispersions of the highest mass AGNs consistent with the upper limit on σ_{*} in the nearby universe and requires a steepening of the $M_{\bullet}-\sigma_{*}$ relationship for the most massive galaxies. The dispersion about the $M_{\bullet}-\sigma_{*}$ rela-

tionship decreases as the mass of black holes increases. The tightness of the relationship for the most massive AGNs provides strong support both for the reliability of the proposed $\text{FWHM}_{[O III]}$ to σ_{*} transformation and of the Dibai method of estimating black hole masses from single-epoch spectra of type-1 AGNs. There is no evidence yet evolution of the $M_{\bullet}-\sigma_{*}$ relationship from $z \sim 3$ to the present day but much further work on this is needed with better-defined samples.

I would like to thank John Kormendy for major encouragement during the course of this investigation, and Sandy Faber, Karl Gebhardt, Jenny Greene, Phil Hopkins, Sarah Salviander, Greg Shields, Remco van den Bosch, and Bev Wills for helpful discussions. This research has been supported in part by the US National Science Foundation through grant AST 08-03883.

REFERENCES

- Bentz, M. C., Peterson, B. M., Pogge, R. W., & Vestergaard, M. 2009b, *ApJ Letts.*, 694, L166
- Bentz, M. C., Peterson, B. M., Netzer, H., Pogge, R. W., & Vestergaard, M. 2009, *ApJ*, 697, 160
- Bernardi, M., Hyde, J. B., Sheth, R. K., Miller, C. J., & Nichol, R. C. 2007, *AJ*, 133, 1741
- Bernardi, M., Sheth, R. K., Tundo, E., & Hyde, J. B. 2007, *ApJ*, 660, 267
- Bochkarev, N. G., & Gaskell, C. M. 2009, *Ast. Lett.*, 35, 287
- Bonning, E. W., Shields, G. A., Salviander, S., & McLure, R. J. 2005, *ApJ*, 626, 89
- Boroson, T. A. 2003, *ApJ*, 585, 647
- Brotherton, M. S. 1996a, Ph.D. Dissertation, University of Texas at Austin (B96a)
- Brotherton, M. S. 1996b, *ApJS*, 102, 1 (B96b)
- Burbidge, E. M., Burbidge, G. R., & Prendergast, K. H. 1959, *ApJ*, 130, 26
- Cherepashchuk, A. M., & Lyutyi, V. M. 1973, *Astrophys. Lett.*, 13, 165
- Dasyra, K. M., et al. 2007, *ApJ*, 657, 102
- Denney, K. D., Peterson, B. M., Dietrich, M., Vestergaard, M., & Bentz, M. C. 2009, *ApJ*, 692, 246
- De Robertis, M. M., & Osterbrock, D. E. 1986, *ApJ*, 301, 727
- Dibai, É. A. 1977, *Soviet Astron. Lett.*, 3, 1
- Dibai, É. A. 1980, *Soviet Astron.*, 24, 389
- Dibai, É. A. 1984b, *Soviet Astron.*, 28, 245
- Dietrich, M., Appenzeller, I., Vestergaard, M., & Wagner, S. J. 2002, *ApJ*, 564, 581
- Ebisuzaki, T., Makino, J., & Okumura, S. K. 1991, *Nature*, 354, 212
- Faber, S. M., & Jackson, R. E. 1976, *ApJ*, 204, 668
- Ferrarese, L., & Merritt, D. 2000, *ApJ*, 539, L9
- Gaskell, C. M. 1988, *ApJ*, 325, 114
- Gaskell, C. M. 2009, *NewA Rev*, in press
- Gaskell, C. M., & Goosmann, R. W., *ApJ*, submitted [arXiv:0805.4258]
- Gaskell, C. M. & Kormendy, J. in *Galaxy Evolution: Emerging Insights and New Challenges*, ed. S. Jogee, L. Hao, G. Blanc, and I. Marinov, ASP Conference Series, in press [arXiv:0907.1652]
- Gaskell, C. M. & Sparke, L. S. 1986, *ApJ*, 305, 175
- Gebhardt, K., et al. 2000, *ApJ*, 539, L13
- Gebhardt, K., & Thomas, J. 2009, *ApJ*, 700, 1690
- Graham, A. W. 2008, *ApJ*, 680, 143
- Greene, J. E., & Ho, L. C. 2005, *ApJ*, 627, 721
- Greene, J. E., & Ho, L. C. 2006, *ApJ*, 641, L21
- Grupe, D., Beuermann, K., Mannheim, K., & Thomas, H.-C. 1999, *A&A*, 350, 805
- Gültekin, K., et al. 2009, *ApJ*, 698, 198
- Hu, J. 2008, *MNRAS*, 386, 2242
- Humphrey, P. J., Buote, D. A., Brighenti, F., Gebhardt, K., & Mathews, W. G. 2008, *ApJ*, 683, 161
- Isobe, T., Feigelson, E. D., Akritas, M. G., Babu, G. J., 1990, *ApJ*, 364, 104
- Koratkar, A. P. & Gaskell, C. M. 1989, *ApJ*, 345, 637
- Kormendy, J., & Bender, R. 2009, *ApJ*, 691, L142
- Kormendy, J., Fisher, D. B., Cornell, M. E., & Bender, R. 2009, *ApJS*, 182, 216
- Kormendy, J., & Gebhardt, K. 2001, in *20th Texas Symposium on Relativistic Astrophysics*, ed. J. C. Wheeler and H. Martel. AIP Conf. Proc., 586, 363
- Kormendy, J., & Kennicutt, R. C., Jr. 2004, *ARA&A*, 42, 603
- Lauer, T. R., et al. 2007, *ApJ*, 662, 808
- Lyutyi, V. M. & Cherepashchuk, A. M. 1972, *Astron. Tsirk*, 688, 1
- McIntosh, D. H., Rieke, M. J., Rix, H.-W., Foltz, C. B., & Weymann, R. J. 1999, *ApJ*, 514, 40
- Nelson, C. H. 2000, *ApJ*, 544 L91
- Nelson, C. H., Green, R. F., Bower, G., Gebhardt, K., & Weistrop, D. 2004, *ApJ*, 615, 652
- Nelson, C. H. & Whittle, M. 1995, *ApJS*, 99, 67
- Nelson, C. H. & Whittle, M. 1996, *ApJ*, 465, 96
- Oegerle, W. R., & Hoessel, J. G. 1991, *ApJ*, 375, 15
- Onken, C. A., Ferrarese, L., Merritt, D., Peterson, B. M., Pogge, R. W., Vestergaard, M., & Wandel, A. 2004, *ApJ*, 615, 645
- Phillips, M. M., Jenkins, C., Dopita, M. A., Sadler, E. M., & Binette, L. 1986, *AJ*, 91, 1062
- Rice, M. S., Martini, P., Greene, J. E., Pogge, R. W., Shields, J. C., Mulchaey, J. S., & Regan, M. W. 2006, *ApJ*, 636, 654
- Salviander, S., Shields, G. A., Gebhardt, K., & Bonning, E. W. 2007, *ApJ*, 662, 131
- Salviander, S., Shields, G. A., Gebhardt, K., Bernardi, M., & Hyde, J. B. 2008, *ApJ*, 687, 828
- Shields, G. A., Gebhardt, K., Salviander, S., Wills, B. J., Xie, B., Brotherton, M. S., Yuan, J., & Dietrich, M. 2003, *ApJ*, 583, 124
- Tremaine, S., et al. 2002, *ApJ*, 574, 740
- van den Bosch, R. M. C. 2008, Ph.D. thesis, University of Leiden
- van den Bosch, R. M. C., et al. 2009, *ApJ* submitted
- Vestergaard, M., & Peterson, B. M. 2006, *ApJ*, 641, 689
- Watson, L. C., Martini, P., Dasyra, K. M., Bentz, M. C., Ferrarese, L., Peterson, B. M., Pogge, R. W., & Tacconi, L. J. 2008, *ApJ*, 682, L21
- Woo, J.-H., Treu, T., Malkan, M. A., & Blandford, R. D. 2008, *ApJ*, 681, 925
- Wyithe, J. S. B. 2006, *MNRAS*, 365, 1082